[AMERICAN JOURNAL OF SCIENCE, VOL. 286, FEBRUARY, 1986, P. 81-104]

American Journal of Science

*FEBRUARY 1986*

# THE INFLUENCE OF NaCl AND KCl ON PHASE RELATIONS IN METAMORPHOSED CARBONATE ROCKS

GEORGE SKIPPEN* and VOLKMAR TROMMSDORFF**

**ABSTRACT. Available experimental data have been used to construct a P-T projection of the system NaCl–$CO_2$–$H_2O$ from 0 to 2 kb and up to 1000°C. With the aid of field information, this system has been extended to 6 kb. Chemographic relationships are shown on this P-T projection. The stability fields of carbonate-silicate mineral assemblages from metamorphic rocks have been projected onto the phase elements of the ternary NaCl–$CO_2$–$H_2O$. Dehydration, decarbonation, and mixed volatile reactions that model common isograds of metamorphism in dolomitic marbles are related to the elements halite, halite + vapor, halite + liquid, halite + liquid + vapor, and liquid + vapor. Phase relations are derived on isothermal, isobaric plots of the chemical potentials of $CO_2$ and $H_2O$ and on composition sections in NaCl–$H_2O$–$CO_2$.**

**Studies of primary solid and fluid inclusions in metasomatic veins from Campolungo, Switzerland show that the phase element salt + liquid + vapor for equal molar proportions of NaCl and KCl in the salt is located approximately at T = 500°C; P = 2000 bars; $\ln f_{H_2O} \approx 3.5$; $\ln f_{CO_2} \approx 8.0$.**

## INTRODUCTION

The importance of the fluid phase in the metamorphism of carbonate rocks was indicated by Goldschmidt (1912) in his discussion of the principles of metamorphism. Bowen (1940) also explained the progressive metamorphism of marbles as a process of devolatilization. Korzhinskii (1959) developed the treatment of mixed volatile equilibria in carbonates through the use of chemical potential diagrams which expressed the stability of mineral assemblages as functions of the activities or fugacities of components such as $H_2O$ and $CO_2$. Chemical potential diagrams provide a basis for the discussion of phase relations in the present paper.

Recently, phase relations in marbles have been described on isobaric temperature-mole fraction $CO_2$ diagrams (Wyllie, 1962; Greenwood, 1967). It is usually assumed in the calculation of these diagrams that the partial pressures of $CO_2$ and $H_2O$ sum to a constant value equated with lithostatic pressure or else to a lithostatic pressure that varies with temperature

* Ottawa-Carleton Centre for Geoscience Studies, Carleton University, Ottawa, Canada, K1S 5B6

** Institut für Mineralogie und Petrographie, ETH-Zentrum, CH-8092 Zürich, Switzerland

according to a pressure-temperature gradient (Trommsdorff, 1972; Flowers and Helgeson, 1983). Bruton and Helgeson (1983) have shown that fluid pressure rather than lithostatic pressure controls mineral stability in veins. Recent data from the Kola borehole (Kozlowski, 1984) suggest that fluid pressures might be significantly less than lithostatic pressure to considerable depth in the crust. Hydrostatic pressure may therefore define a lower limit for fluid pressure in high-grade metamorphic rocks.

Calculations based on the assumption that $CO_2$ and $H_2O$ are the significant species in the fluid have provided insight into the metamorphism of carbonate rocks. It has been widely recognized, however, that the composition of the fluid phase is more complex. For example, volatile species such as $CH_4$, CO, $H_2$ have been considered for rocks containing graphite (French, 1966; Eugster and Skippen 1967; Ohmoto and Kerrick, 1977). Many workers have observed substantial concentrations of dissolved species such as $N_2$ (for example, Guilhaumou and others, 1981; Kreulen and Schuiling, 1982) and chlorides in fluid inclusions from metamorphosed carbonates (for example, Poty, Leroy, and Cuney, 1974; Crawford, Kraus, and Hollister, 1979; Kreulen, 1980; Touret, 1981; Sisson, Crawford, and Thompson, 1981). The importance of chlorides as fluid components has also been emphasized by Bowers and Helgeson (1983a, b).

Trommsdorff, Skippen, and Ulmer (1985) have described solid inclusions of halite and sylvite in metamorphosed carbonate rocks. This observation supports evidence that chlorides are important components of metamorphic fluids and also shows that these fluids can be saturated with respect to chloride components under certain circumstances. The present paper examines phase relations in metamorphic fluids containing chloride components and considers the influence of concentrated brines on the stability of mineral assemblages formed during the metamorphism of carbonate rocks.

## P-T PROJECTION OF $NaCl–H_2O–CO_2$

Gehrig (1980) constructed a schematic pressure-temperature projection for $NaCl–H_2O–CO_2$. Existing experimental data can be combined with the schematic projection of Gehrig to construct a quantitative P-T diagram (fig. 1) to 900°C and 2000 bars. Curves above 900°C on figure 1 have not been located experimentally and are shown schematically.

A solid circle on figure 1 indicates the critical point $K_{H_2O}$ in the unary $H_2O$ with the liquid + vapor curve in the unary and the binary critical curves in $H_2O–CO_2$ and $NaCl–H_2O$ coincident at this critical point. The critical curve in the binary $NaCl–H_2O$ has been measured to 700°C by Sourirajan and Kennedy (1962). The critical curve in $H_2O–CO_2$ has been investigated to 3500 bars by Todheide and Franck (1963) and Takenouchi and Kennedy (1964).

The solid square on figure 1 indicates the triple point $T_{NaCl}$ of NaCl with the unary melting and liquid + vapor curves as well as the binary curves for liquid + vapor + halite coincident at this point. The three-phase curve liquid + vapor + halite in $NaCl–H_2O$ has been measured to

708.5°C by Sourirajan and Kennedy (1962). The three-phase curve liquid + vapor + halite has not yet been determined in NaCl–$CO_2$ and is located schematically on figure 1. The unary melting curve in NaCl has been measured to 65 kb by Akella, Vaidya, and Kennedy (1969). Solubilities of $CO_2$ in liquid NaCl have been measured by Grjotheim and coworkers (1962) at 1 atm of $CO_2$ pressure between 810° and 950°C indicating that the unary liquid + vapor curve in NaCl exists at less than 1 atm over these temperatures. The critical point for the unary NaCl has not been determined. The three curves at high temperature in figure 1, that is, the unary liquid + vapor curve in NaCl and the binary critical curves in NaCl–$H_2O$ and NaCl–$CO_2$ must all meet at the critical point for NaCl, as indicated schematically on figure 2.

The experimentally determined curves on figure 1 indicate that the pressure-temperature relationships in NaCl–$H_2O$–$CO_2$ are reasonably well understood at low pressures. Quantitative phase relations are less well established at higher pressures, although an understanding of the ternary system at higher pressures is essential for the study of metamorphic rocks

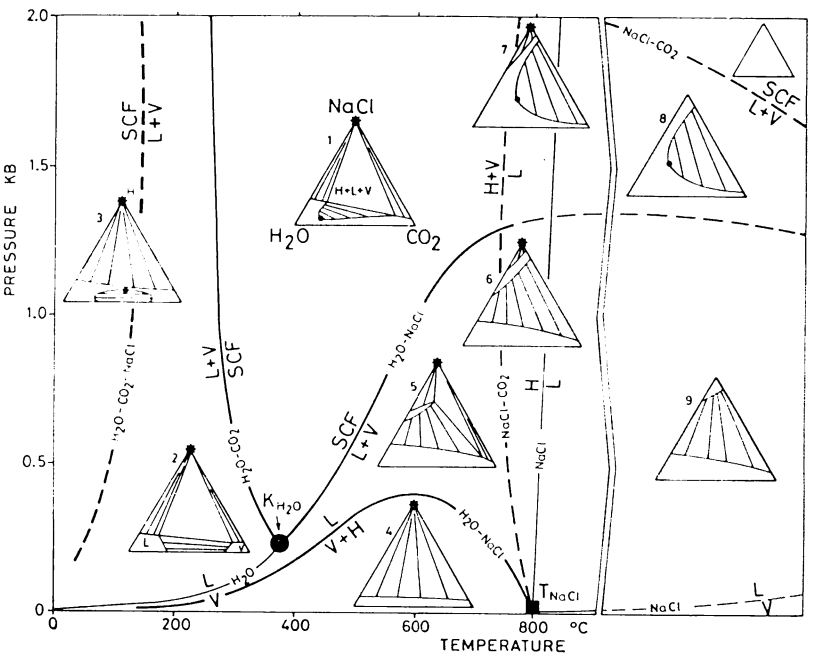


Fig. 1. Pressure-temperature projection for the ternary system NaCl–$H_2O$–$CO_2$. Unary curves with a thin signature, binary curves with an intermediate thickness, a portion of the ternary supercritical curve with a heavy signature. The experimentally measured parts of curves are solid, and estimated curves are dashed. A scale-break is indicated at 900°C as the position of curves above 900°C is speculative. All three curves extrapolated above 900°C meet at the experimentally undetermined critical point for NaCl. Chemographic relationships are shown schematically. L = liquid, V = vapor, H = * = halite, SCF = supercritical fluid, $K_{H_2O}$ = critical point for $H_2O$, $T_{NaCl}$ = triple point for halite, liquid, vapor in the unary, NaCl.

equilibrated in the presence of saline fluids. It is particularly important to establish the boundaries between the two-phase region of liquid–vapor and the region of supercritical fluid, since phase relations and geologic processes such as mass transfer depend on the physical nature of the fluids present.

Ternary critical fluids are bounded by critical phenomena in the binary $NaCl–CO_2$ at points P and Q on figure 2. Point Q lies above the maximum pressure of figure 2, and those curves labelled Q are coincident at a single point above the maximum pressure of the diagram. Points P and Q correspond to the intersections of the binary critical curve for the system $NaCl–CO_2$ with the ruled surface on which liquid + vapor + halite coexist in this binary. Gehrig (1980) has indicated that point P in $NaCl–CO_2$ must be close to the critical point of $CO_2$ because of the limited solubility of NaCl in $CO_2$-rich fluids. As $H_2O$ is added to $NaCl–CO_2$, a family of points in the ternary system, corresponding to P and Q in the binary, defines a ternary critical curve shown with a heavy dashed signature on figure 2. This ternary critical curve, PQ, has not yet been located ex-

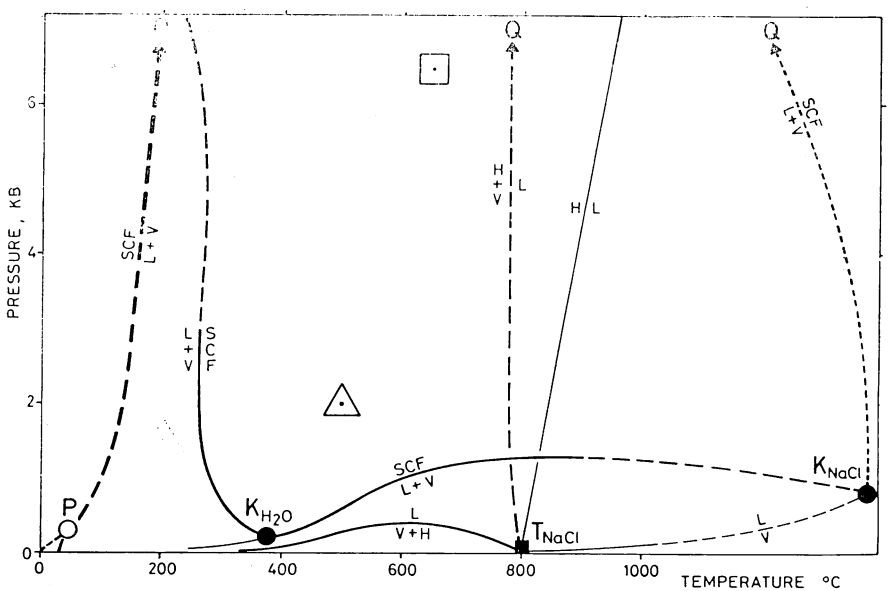


Fig. 2. Pressure-temperature projection for the ternary system $NaCl–H_2O–CO_2$. Unary curves with a thin signature, binary curves with an intermediate thickness, a portion of the ternary supercritical curve shown with a heavy signature. The experimentally measured parts of curves are solid and estimated curves are dashed. Those curves ending at point Q are coincident at a single point, Q, at a pressure greater than shown in the diagram. The square represents a point determined by Sisson and others (1982) for coexisting brine + vapor during the formation of fluid inclusions in metamorphic rocks developed at 600°C and 6.5 kb. The triangle corresponds to the pressure and temperature estimated by Mercolli (1982) for coexisting liquid + vapor at Campolungo, Switzerland. H = halite, L = liquid, SCF = supercritical fluid, $K_{H_2O}$ = critical point in the unary system, $H_2O$, $T_{NaCl}$ = triple point for halite, liquid, vapor in the unary, NaCl, $K_{NaCl}$ = schematically located critical point in NaCl.

perimentally; its position must therefore be estimated on the basis of the limited experimental data available for the ternary system as well as field evidence.

Takenouchi and Kennedy (1965) have measured the solubility of $CO_2$ in brines at temperatures down to 150°C and pressures to 1400 bars. These data indicate that liquids saturated with $CO_2$ have a decreasing solubility of $CO_2$ with increasing NaCl (to 20 wt percent) as suggested by triangle 2 on figure 1. A point at 150°C and 1400 bars (figs. 1 and 2) is therefore assumed to lie within the two-phase region liquid + vapor in the ternary.

Sisson, Crawford, and Thompson (1981) have presented evidence for two coexisting fluids in rocks formed apparently at 6.5 kb and 600°C, as indicated by the square on figure 2. $CO_2$-rich fluid inclusions in these rocks coexist with salt-saturated aqueous inclusions as would be consistent with the phase relations shown in triangle 1 on figure 1. The point on figure 2 corresponding to the observations of Sisson and coworkers must therefore lie within the ternary two phase region liquid + vapor. According to these observations phase relations in metamorphosed carbonates will be influenced by coexisting liquid and vapor to high temperatures and pressures.

## PHASE RELATIONS ON CHEMICAL POTENTIAL DIAGRAMS

In describing phase relations for carbonate rocks metamorphosed in the presence of saline fluids, it is helpful to consider relationships among mineral assemblages as functions of the chemical potentials of $CO_2$ and $H_2O$ as well as composition diagrams for the fluids. Mineral equilibria are represented by linear relationships on chemical potential diagrams but exhibit more complex relationships when composition is given explicitly as on isothermal, isobaric ternary composition sections. The composition diagrams, however, have the advantage of providing a more direct indication of the physical nature of the fluid.

The phase elements on a typical composition diagram (triangle 1) occupying an important part of P-T space on figure 1 are shown schematically in the composition diagram of figure 3A and the chemical potential diagram of figure 3B. Unary elements are labelled on both diagrams with letters, binary elements with numbers, and ternary with Roman numerals. The stable phase in each of the unary systems $H_2O$ and $CO_2$ plots along the ordinate and abscissa, respectively, of the chemical potential diagram. The stable phase in the unary NaCl is represented by the origin on figure 3B.

Binary systems NaCl–$H_2O$ (labelled 1) and NaCl–$CO_2$ (labelled 2) plot as straight lines between the corresponding unaries in chemical potential space as well as composition space. The binary system $H_2O$–$CO_2$ follows a curved path (labelled 3) with the sum of the chemical potentials of $CO_2$ and $H_2O$ related to lithostatic pressure (Skippen, 1974) or hydrostatic pressure (Bruton and Helgeson, 1983) or some other geologically interesting condition.

All ternary phase relations are shown on figure 3 within the area bounded by the binary systems. This is not, however, a necessary condition

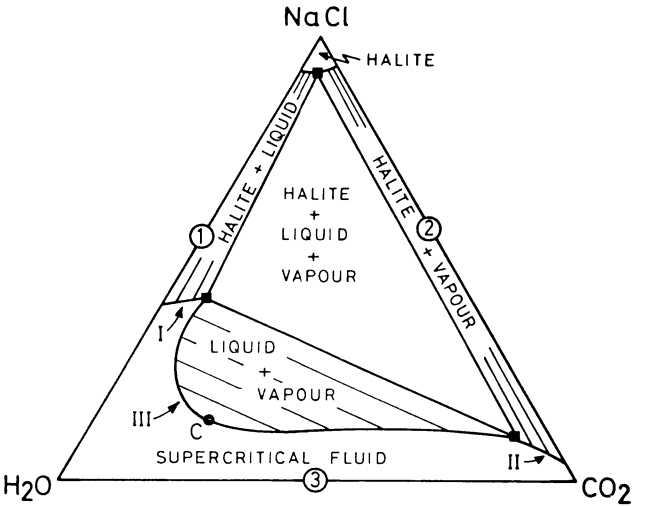


A.

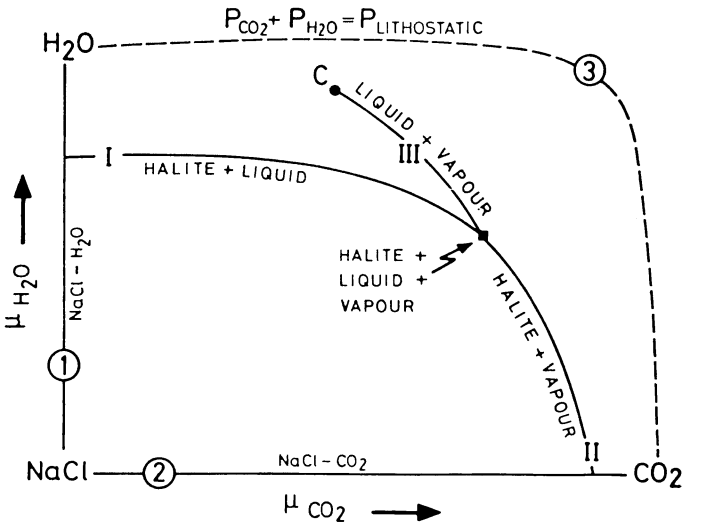


B.

Fig. 3. Phase elements in $NaCl–H_2O–CO_2$ shown schematically for that region of pressure-temperature space in which the ternary phase element halite + liquid + vapor is stable with a supercritical fluid in the binary $H_2O–CO_2$. Binary elements are indicated with numbers, and ternary elements with Roman numerals. C = consolute point. The boundary of the ternary liquid + vapor region has been studied by Gehrig (1980) and Bowers and Helgeson (1983a). (A) Isobaric isothermal composition section. (B) Chemical potential of $CO_2$ versus chemical potential of $H_2O$.

in chemical potential space, where excess chemical potentials for $CO_2$ or $H_2O$ could result in stable ternary elements outside the area bounded by the binaries. Among the ternary elements that can be represented on the chemical potential diagram are the lines corresponding to the saturation of fluids with halite. The liquid + halite line (curve I) extends from the binary system NaCl–$H_2O$ and the vapor + halite line (curve II) from NaCl–$CO_2$ toward the three-phase region halite + liquid + vapor in the ternary system. The three-phase region in figure 3B plots as a point at the junction of curves I and II, since the criteria for equilibrium require that the chemical potentials of all components be equal in all phases. Curve III corresponds to the coexistence of an $H_2O$-rich liquid and a $CO_2$-rich vapor. This curve on figure 3B extends from the three-phase region to the consolute point, labelled C, at which liquid and vapor become indistinguishable. The two limbs of the liquid + vapor curve extending from the consolute point toward the three-phase region on figure 3A are reduced to a single line on figure 3B because of the equality of chemical potentials in coexisting phases.

The relationship between composition and chemical potential diagrams can be similarly represented for all the topologies on figure 1. These relationships have been summarized on figure 4.

## MINERAL EQUILIBRIA

Various types of equilibria involving volatile components such as $CO_2$ and $H_2O$ can be distinguished (Greenwood, 1967). For example:

1. Dehydration
2. Decarbonation
3. $CO_2$ and $H_2O$ on opposite sides of the equilibrium
4. $CO_2$ and $H_2O$ on the same side of the equilibrium

A series of isotherms (that is, isothermal equilibrium lines) for these types of equilibria are shown on schematic chemical potential diagrams on figures 5 to 8. The binary and ternary curves in NaCl–$H_2O$–$CO_2$ are dependent on pressure and temperature but have been shown as single curves on figures 5 to 8 for simplicity.

Isotherms for a dehydration reaction are shown on figure 5. These isotherms are horizontal lines on figure 5A, since the equilibrium constant for a dehydration equilibrium is independent of $CO_2$. The intercept on the $H_2O$ axis can be calculated from thermodynamic or experimental determinations of the equilibrium constant. At T1 on figure 5A, it can be seen that the isotherm intersects both the binary phase element $H_2O$–$CO_2$ and the ternary curve corresponding to vapor + halite. The T1 isotherm then remains beneath the halite saturation line which is represented in figure 5B by halite solid solutions with $CO_2$ and $H_2O$; the area representing the solid phase has been enlarged on 5B for purposes of illustration.

Isotherm T2 intersects the halite saturation lines at the three-phase element. The intersection of T3 with the element liquid + vapor on 5A results in two phases joined by a tie-line across the liquid + vapor element on 5B. T4 encounters the liquid + vapor element at the consolute com-

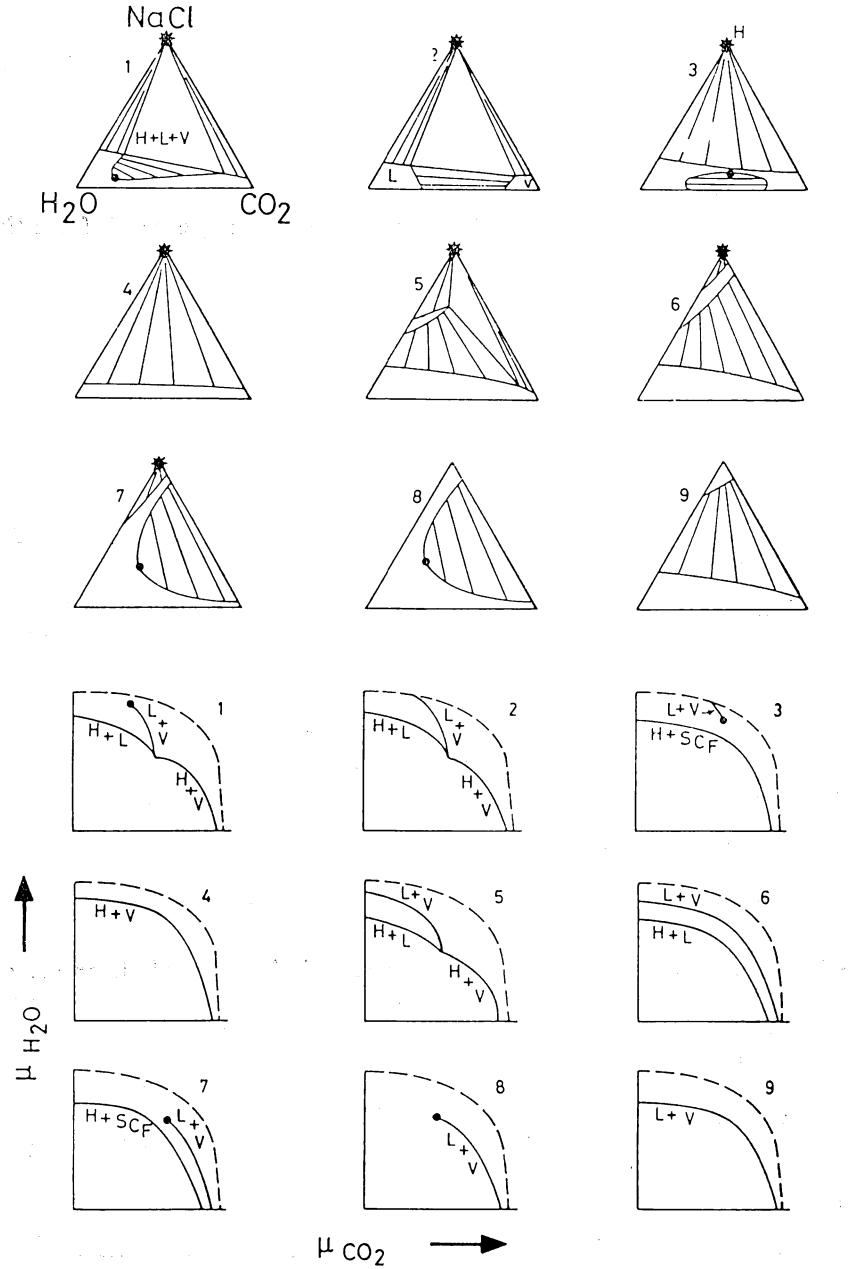


Fig. 4. Relationships between ternary composition sections in $NaCl–H_2O–CO_2$ and phase elements on plots of chemical potential of $H_2O$ versus the chemical potential of $CO_2$. The regions of pressure–temperature space corresponding to each of these diagrams are shown in figure 1. The dashed curve on the chemical potential diagrams represents the binary $H_2O–CO_2$. The mutual solubilities of $CO_2$ and NaCl have been exaggerated for purposes of illustration. H = * = halite, L = liquid, V = vapor, SCF = supercritical fluid. Full circle indicates consolute point. The equilibria and transitions from figure 1 that relate composition sections 1 to 9 are: (1-2) SCF → L + V ($H_2O–CO_2$); (2-3) L + V → SCF ($H_2O–CO_2$–NaCl); (3-4) SCF → L + V ($H_2O–CO_2$–NaCl), L = V ($H_2O$), L = V + H ($H_2O$–NaCl); (4-5) H + V = L ($H_2O$–NaCl); (5-6) H + V = L ($NaCl–CO_2$); (6-7) L + V → SCF ($H_2O$–NaCl); (7-8) H = L (NaCl); (8-9) SCF → L + V ($H_2O$–NaCl).

position. No intersection with the binary NaCl–$CO_2$ is possible on figure 5 for a dehydration equilibrium.

Figure 6 illustrates a series of isotherms on a chemical potential and composition diagram for a decarbonation reaction. The relationship of the decarbonation isotherms to the phase elements in NaCl–$H_2O$–$CO_2$ is comparable to the dehydration equilibrium except that the binary NaCl–$H_2O$ is avoided because the chemical potential of $CO_2$ is undefined on this join.

A mineral equilibrium with $CO_2$ and $H_2O$ on opposite sides is illustrated in figure 7. Isotherms for such an equilibrium fall along curves with varying chemical potentials of both $CO_2$ and $H_2O$. Intersections with either NaCl–$H_2O$ or NaCl–$CO_2$ are impossible, and the isotherms therefore approach the NaCl apex.

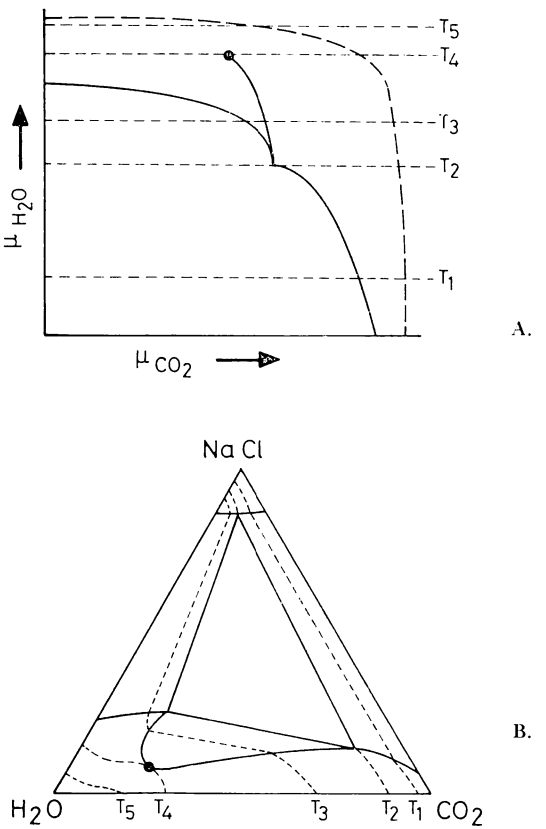


Fig. 5. Schematic isotherms for dehydration equilibria. The isotherms are indicated by lines with a short dash labelled T1 to T5. Phase elements in the ternary system NaCl–$H_2O$–$CO_2$ are as shown on figure 3. (A) chemical potential of $CO_2$ versus chemical potential of $H_2O$. (B) composition section through the ternary system NaCl–$H_2O$–$CO_2$.

Figure 8 illustrates a somewhat more complicated pattern for isotherms describing equilibria with two volatile components on the same side of the equilibrium. As shown by Greenwood (1967), these equilibria have two intersections with the binary $CO_2$–$H_2O$ and terminate at a temperature maximum corresponding to isotherm T4 on figure 8. The nature and number of intersections with the ternary phase elements depend on the slope of the isotherm on 8A relative to the ternary curves. For the isotherms as drawn on figure 8A, the equilibrium intersects the halite saturation lines at four points along T1. This number of intersections could be reduced if the slope of the isotherm on 8A were different. Between the two intersections of T1 with the binary $H_2O$–$CO_2$ on figure 8A, the isotherm intersects the ternary halite + liquid, liquid + vapor, and halite + vapor elements. These intersections result in a complex pattern

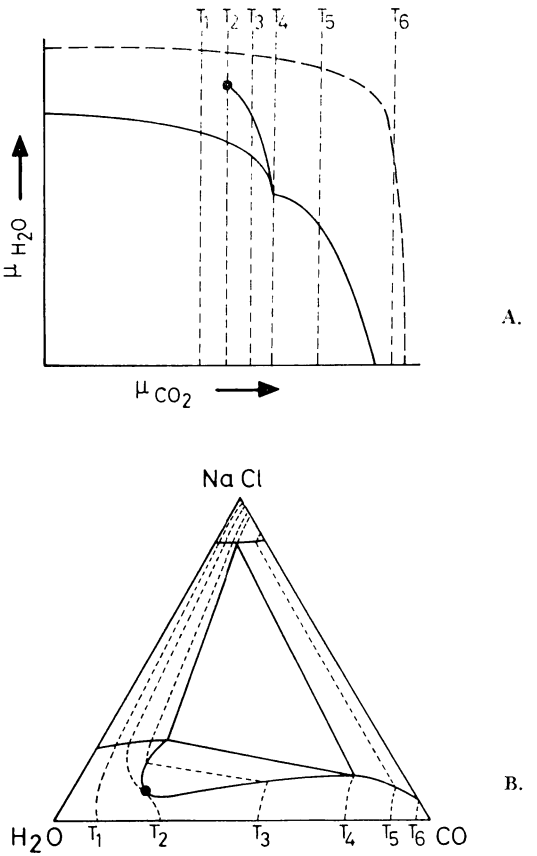


Fig. 6. Schematic isotherms for decarbonation equilibria. The isotherms are indicated by lines with a short-dash labelled T1 to T6. Phase elements in the ternary system NaCl–$H_2O$–$CO_2$ are as shown on figure 3. (A) chemical potential of $CO_2$ versus chemical potential of $H_2O$. (B) Composition section through the ternary system NaCl–$H_2O$–$CO_2$.

for the isotherm on figure 8B. The remainder of the isotherms are shown on figure 8C.

Isotherm T3 is unique in corresponding to a temperature maximum for the mineral equilibrium along the ternary vapor + liquid element. According to Bowers and Helgeson (1983a) a part of the L + V element may lie outside the binary $CO_2$–$H_2O$ on figure 8A (compare fig. 9). The point $T_4$ could then be located on the boundary of L + V.

## RELATIONSHIPS BETWEEN MINERAL ASSEMBLAGES AND TERNARY FLUIDS

Phase relations in calcite-bearing metacarbonates can be described by reference to the following 6-phase assemblages (Skippen, 1974):

I: talc, tremolite, calcite, dolomite, quartz, fluid
II: tremolite, diopside, calcite, dolomite, quartz, fluid
III: tremolite, diopside, forsterite, calcite, dolomite, fluid.

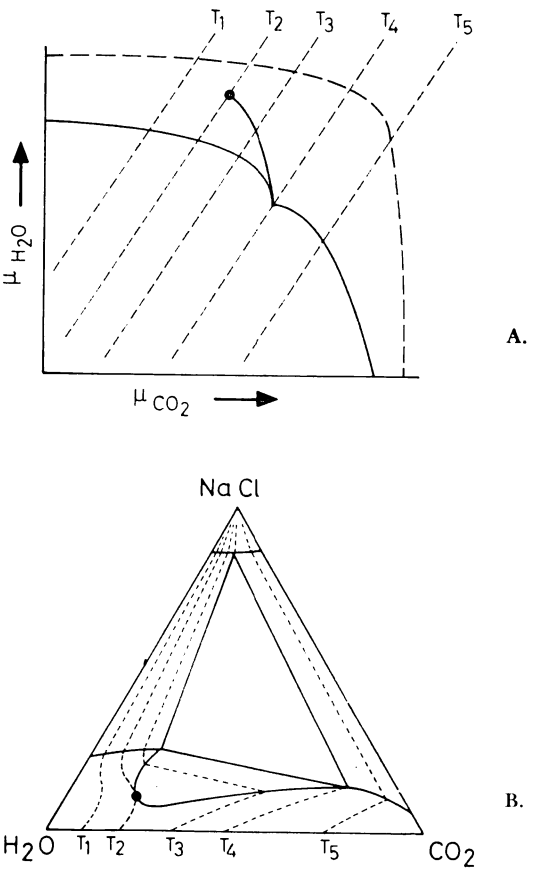


Fig. 7. Schematic isotherms for mixed volatile equilibria with $CO_2$ and $H_2O$ on opposite sides. The isotherms are indicated by lines with a short dash labelled T1 to T5. Phase elements in the ternary system NaCl–$H_2O$–$CO_2$ are as shown on figure 3. (A) chemical potential of $CO_2$ versus chemical potential of $H_2O$. (B) composition section through the ternary system NaCl–$H_2O$–$CO_2$.

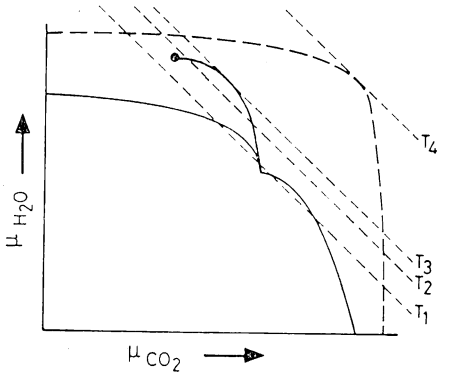


A.

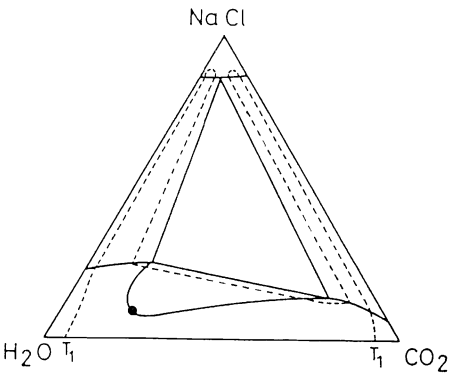


B.

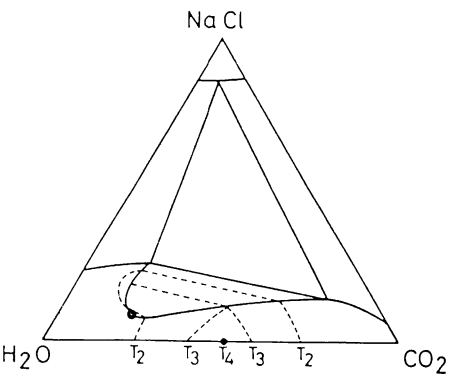


C.

Fig. 8. Schematic isotherms for mixed volatile equilibria with $CO_2$ and $H_2O$. on the same side. The isotherms are indicated by lines with a short dash labelled T1 to T4. Phase elements in the ternary system NaCl–$H_2O$–$CO_2$ are as shown on figure 3. (A) chemical potential of $CO_2$ versus chemical potential of $H_2O$. (B, C) composition sections through the ternary system NaCl–$H_2O$–$CO_2$.

Points indicating the stability of the above assemblages are plotted on figure 9 using thermodynamic data from Helgeson and coworkers (1978). These assemblages are connected, where appropriate, with lines representing common four-mineral elements.

Fluids in the binary system $H_2O$–$CO_2$ under lithostatic pressure are represented in figures 9 and 10 by a curve calculated with fugacity coefficients from Bowers and Helgeson (1983a). These authors calculated the coefficients with the modified Redlich-Kwong equation of state as proposed by Holloway (1977) and modified by Flowers (1979).

A curve representing the coexistence of liquid + vapor in the ternary system NaCl–$H_2O$–$CO_2$ is plotted on figures 9 and 10 using fugacity data from Bowers and Helgeson (1983a; figs. 30, 31). The curve for the ternary liquid + vapor element plots outside the binary lithostatic line in $H_2O$–

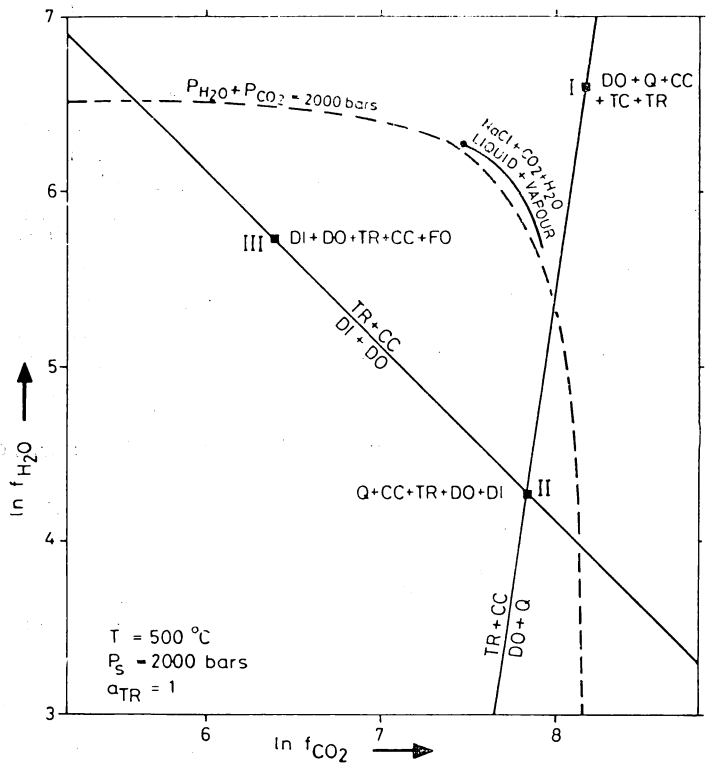


Fig. 9. Natural logarithms of the fugacities of $H_2O$ and $CO_2$ at 500°C and 2000 bars. The dashed curve represents the binary supercritical fluid in $H_2O$–$CO_2$. The solid curve represents the liquid + vapor element in the ternary system NaCl–$H_2O$–$CO_2$ as calculated by Bowers and Helgeson (1983a). The straight lines indicate mixed volatile equilibria which connect the following 5-mineral assemblages (point I: talc, tremolite, dolomite, calcite, quartz) (point II: tremolite, diopside, dolomite, calcite, quartz) (point III: forsterite, diopside, tremolite, dolomite, calcite).

$CO_2$ due to the excess chemical potentials of $CO_2$ and $H_2O$ calculated by Bowers and Helgeson.

Halite saturation lines have been used in the discussion above to model the saturation of fluids with salt components. In geologic fluids, however, the dissolved chlorides include KCl and $CaCl_2$ as well as NaCl (Trommsdorff and others, 1985). The chemical potential of $H_2O$ is lowered considerably in a liquid saturated with respect to both NaCl and KCl in comparison to a liquid saturated with a single salt. An indication of this effect is seen in the melting temperature of 660°C (Chou, 1982) for crystals with equal molar proportions of KCl and NaCl at 1 atm compared to 800.5°C for pure NaCl. The salt saturation lines on figure 10 are therefore plotted at lower chemical potentials of $H_2O$ for KCl–NaCl mixtures.

Free energies have not yet been measured for salt-saturated fluids at the conditions of interest in this study. It is, however, possible to obtain some indication of the position of the salt saturation lines on figure 10. They are bracketed at higher chemical potentials by the binary lithostat and at lesser chemical potentials by evidence from field relations at Campolungo, as described below.

### EVIDENCE FROM THE FLUID AND SOLID INCLUSIONS AT CAMPOLUNGO

The development of metasomatic quartz–calcite–tremolite veins in the dolomitic marbles of Campolungo, Switzerland has been described by Walther (1983). The fluid inclusions in these veins have been thoroughly studied by Mercolli (1982) with additional information provided by Walther. Mercolli has recognized several generations of fluid inclusions, the most significant of which for the genesis of the tremolite veins is the earliest. This set consists of two types with the properties measured by Mercolli (ms) summarized in table 1; aqueous inclusions contain approx 50 wt percent NaCl plus KCl and now contain a salt crystal at room temperature. Always associated with these saline aqueous inclusions is a second type containing more than 90 percent by volume $CO_2$. J Touret (personal commun, June, 1985) considers that less than 10 percent of other gases does not significantly alter the volumetric properties of $CO_2$. Mercolli has carefully examined the question of whether or not the saline aqueous and $CO_2$-rich inclusions truly represent coexisting fluids. He has concluded that the two fluids were coexisting at the time of entrapment on the basis of geometric relationships within single fractures. Mercolli has observed that these two types of fluid inclusion are related spatially

TABLE 1

Early, cogenetic fluid inclusions in sample B1B (Mercolli, 1979)

| | Multiphase inclusions | $CO_2$-rich inclusions |
|---|---|---|
| volume percent $CO_2$ | 5 | 90 - 95 |
| wt percent NaCl | 42 - 50 | n.d. |
| T(C), homogenization NaCl | 495.6 - 498.2 | — |
| T(C), homogenization $CO_2$ | — | 26.9 - 28.9 |
| T(C), fusion $CO_2$ | — | (–56.6) - (–58.6) |
| diameter of inclusions, $\mu$m | 10 | 10 |

to the tremolite veins. He has concluded that fluids represented by these inclusions are related to the genesis of the veins.

The maximum temperature for the dissolution of salt crystals in the aqueous inclusions described by Mercolli (ms) is near 500°C. This agrees well with calcite-dolomite thermometry of the veins by Mercolli and by Walther (1983) who obtained temperatures of 500° ± 20°C from magnesian calcite compositions. Isochores determined from homogenization temperatures (Mercolli, 1982) indicate a pressure of 2000 bars at 500°C. Walther has estimated a higher pressure of 3.25 kb. The consistency of temperature determinations from calcite-dolomite geothermometry and the salt dissolution measurements by Mercolli support the hypothesis that the fluids were in equilibrium with chloride minerals at the time the vein minerals formed. This possibility has been enhanced by the observations of Trommsdorff, Skippen, and Ulmer (1985) who discovered apparently primary solid inclusions of halite and sylvite in the vein minerals at Campolungo containing the saturated fluid inclusions. The compositions of coexisting halite and sylvite in these primary salt inclusions also indicate a temperature of 500°C when compared with the miscibility gap in the system KCl–NaCl.

The equilibrium mineral assemblage places the veins on the reaction line, dolomite + quartz + calcite + tremolite + fluid. The stable portion of this reaction line on figures 10 and 11 is between points I′ and II′ where talc or diopside, respectively, are added to that assemblage. The position of the reaction line and points I′ and II′ have been calculated for figures 10 and 11 using data from Helgeson and coworkers (1978). The reaction line has been adjusted for impurities in the tremolite (see table 2), using an ideal solution model for amphibole (Skippen and Carmichael, 1977). The analytical data in table 2 indicate an OH–tremolite component activity of 0.27. It may be noted that points I′ and II′ (figs. 10, 11) involving this impure amphibole differ from the corresponding points on figure 9 for pure tremolite.

It is possible to constrain further the vein assemblage to a point along the reaction line, if the mole fraction of $CO_2$ in the vapor is used to calculate the equilibrium fugacity of $CO_2$. The method described by Burruss (1981, p. 61) has been used to calculate a minimum $CO_2$ content of 70 mole percent for the $CO_2$-rich inclusions, using data given in table 1. Fugacity coefficients for mixtures in $NaCl–H_2O–CO_2$, as calculated by Bowers and Helgeson (1983a), have been used to locate specific fluid compositions along the reaction line in figures 10 and 11.

Two additional observations enable phase relations in the system $NaCl–KCl–H_2O–CO_2$ to be correlated with the carbonate veins from Campolungo. Mercolli (1982) observed that salt crystals in the primary generation of aqueous liquid inclusions were completely redissolved at temperatures between 495.6° and 498.2°C, that is, the temperature of formation of the veins as independently determined from calcite-dolomite geothermometry. This indicates that the primary liquid was saturated with respect to salt components. Furthermore, Trommsdorff, Skippen,

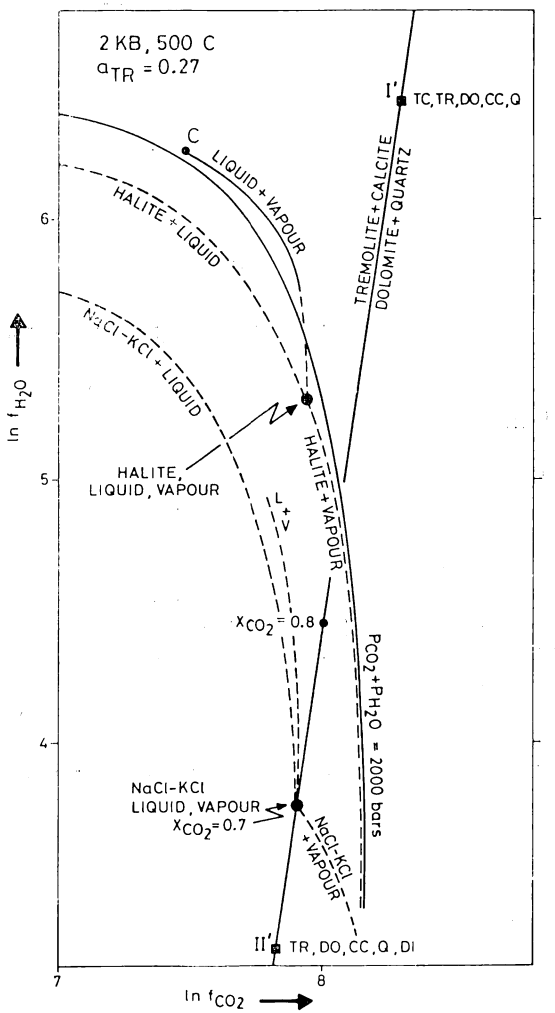


Fig. 10. Natural logarithms of the fugacities of $H_2O$ and $CO_2$ at 2000 bars and 500°C. The diagram applies to metasomatic tremolite–quartz–calcite veins in dolomitic marbles at Campolungo, Switzerland. The ternary liquid + vapor element ends at consolute point C and plots above the binary curve for supercritical fluids in $H_2O$–$CO_2$. The solid portion of the ternary liquid + vapor element indicates that part of this element has been plotted from the data of Bowers and Helgeson (1983a). The dashed portion of this curve as well as the halite + liquid and the halite + vapor elements are estimated. The point labelled NaCl–KCl–vapor is located by phase assemblages observed in the rocks of Campolungo. The estimated positions of the remaining phase elements in NaCl–KCl–$H_2O$–$CO_2$ are shown in a dashed pattern. The straight line connecting points I′ and II′ represents the equilibrium position of the assemblage, tremolite–quartz–calcite–dolomite as observed in the rocks from Campolungo. Points I′ and II′ indicate the equilibrium positions calculated for the 5-phase assemblages, talc–tremolite–dolomite–calcite–quartz and tremolite–diopside–dolomite–calcite–quartz. The positions along the equilibrium line for mole fractions of $CO_2(X_{CO_2})$ in the supercritical fluid of 0.8 and 0.7 are also indicated; these points were calculated using fugacity coefficients for NaCl–$H_2O$–$CO_2$ from Bowers and Helgeson (1983a). C = consolute point, L = liquid, V = vapor.

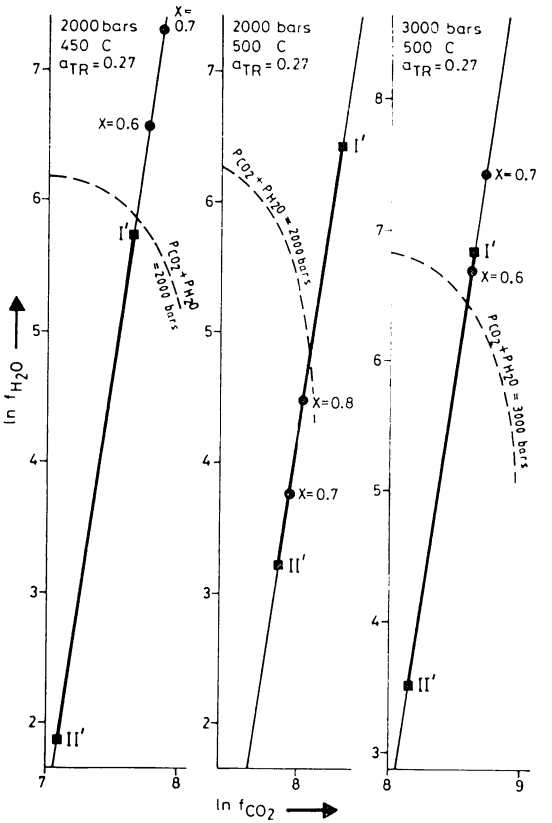


Fig. 11. Natural logarithms of the fugacity of $CO_2$ and $H_2O$. Curves and lines are as described for figure 10. The calculated position of the mole fraction of $CO_2$ (X) for various compositions of the supercritical fluid in NaCl–$H_2O$–$CO_2$ are indicated by points along the equilibrium line. Fugacity coefficients from Bowers and Helgeson were used to calculate the fluid compositions. (A) 2000 bars, 450°C. (B) 2000 bars, 500°C. (C) 3000 bars, 500°C.

TABLE 2

Microprobe analysis of tremolite, sample B1B

| | Wt percent | |
|---|---|---|
| $SiO_2$ | 58.02 | Cl < .02 |
| $TiO_2$ | 0.03 | $Cr_2O_3$ < .03 |
| $Al_2O_3$ | 1.26 | MnO n.d. |
| FeO | 0.15 | NiO n.d. |
| MgO | 24.61 | |
| CaO | 13.04 | |
| $Na_2O$ | 0.40 | |
| $K_2O$ | 0.14 | |
| F | 1.66 | |

Average of 15 analyses

$Na_{0.11}\ K_{0.025}\ Ca_{1.92}\ Mg_{4.69}\ Al_{0.21}\ Fe_{0.02}\ Si_8\ O_{22}\ (OH)_{0.65}\ F_{0.35}$

Formula calculated from the analysis with all F associated with Mg

Analyst: P. Ulmer

and Ulmer (1985) have described primary solid inclusions of halite and sylvite from Campolungo vein specimens as independent evidence of the saturation of primary fluids with salt components. The coexisting liquid and vapor inclusions observed by Mercolli together with the evidence for saturation of the fluids with respect to NaCl and KCl indicate that the phase element halite + sylvite + liquid + vapor is located on figure 10 by the point representing the Campolungo veins. Apart from their coincidence at the conditions of the vein assemblage, it is only possible at present to locate schematically the elements salt + liquid, liquid + vapor, salt + vapor on figure 10.

The sensitivity of the approach to locating phase elements in chemical potential space has been tested by varying pressure and temperature as indicated on figure 11. At 450°C and 2000 bars and also at 500°C and 3000 bars, the composition ($X_{CO_2} = 0.7$) of the $CO_2$-rich vapor indicates a metastable point on the reaction line well outside the stable segment between points I and II. The calculated points for $X_{CO_2} = 0.7$ also fall substantially above the binary lithostat in a region that can be assumed to be mechanically unstable.

Data for ternary phase elements in the system $NaCl–H_2O–CO_2$ are limited to that part of the ternary liquid + vapor curve that can be calculated from the results of Bowers and Helgeson (1983a). The remaining phase elements for this system have been located schematically.

## METACARBONATE PHASE RELATIONS ON FLUID COMPOSITION SECTIONS

Mineralogic data from Campolungo have made it possible to correlate carbonate–silicate mineral assemblages with phase elements in the system $NaCl–KCl–H_2O–CO_2$. To this point, these correlations have been limited to chemical potential space where sufficient experimental and thermodynamic data exist to examine phase relations in a complex natural system. It is also possible to transfer these phase relations to composition sections for the fluid system using the relationships summarized on figures 5 to 8.

Such relationships at 2000 bars and 450°, 500°, 525°C are shown on figures 12 to 14. These figures correspond to pseudoternary sections through $NaCl–KCl–H_2O–CO_2$ at approximately equal molar proportions of NaCl/KCl, as observed for solid minerals at Campolungo (Trommsdorff, Skippen, and Ulmer, 1985). The diagrams have been constructed by utilizing the sequence of reaction curves (Skippen, 1974) around the six-phase points I, II, III, whose relative positions are as shown on figure 9 and by taking into account the intersections of these curves with each of the phase elements in the fluid system plotted on figure 10.

Figure 12 for 450°C includes points I, II, and III. Points II and III are plotted within the field of solid salt corresponding to their location on figure 9 below the salt saturation lines. Phase relations in NaCl–KCl (Waldbaum, 1969) indicate that halite and sylvite may coexist at 450°C but are completely miscible at 500°C and above.

Point I plots within the region of supercritical fluid, as illustrated on figure 11B. The position of point I at nearly equal proportions of $CO_2$/

$H_2O$ is consistent with its intersection with the binary $H_2O$–$CO_2$ line at 460°C and $X_{CO_2} = 0.5$ (Walther and Helgeson, 1980). The intersections of reaction curves with $H_2O$–$CO_2$ have also been taken from Walther and Helgeson.

Figures 13 and 14 include only points II and III and associated reaction curves. Point I has passed beyond the binary lithostat in chemical potential space and is therefore unstable at the conditions of these diagrams. Intersections with the $H_2O$–$CO_2$ binary have been taken from Walther and Helgeson (1980).

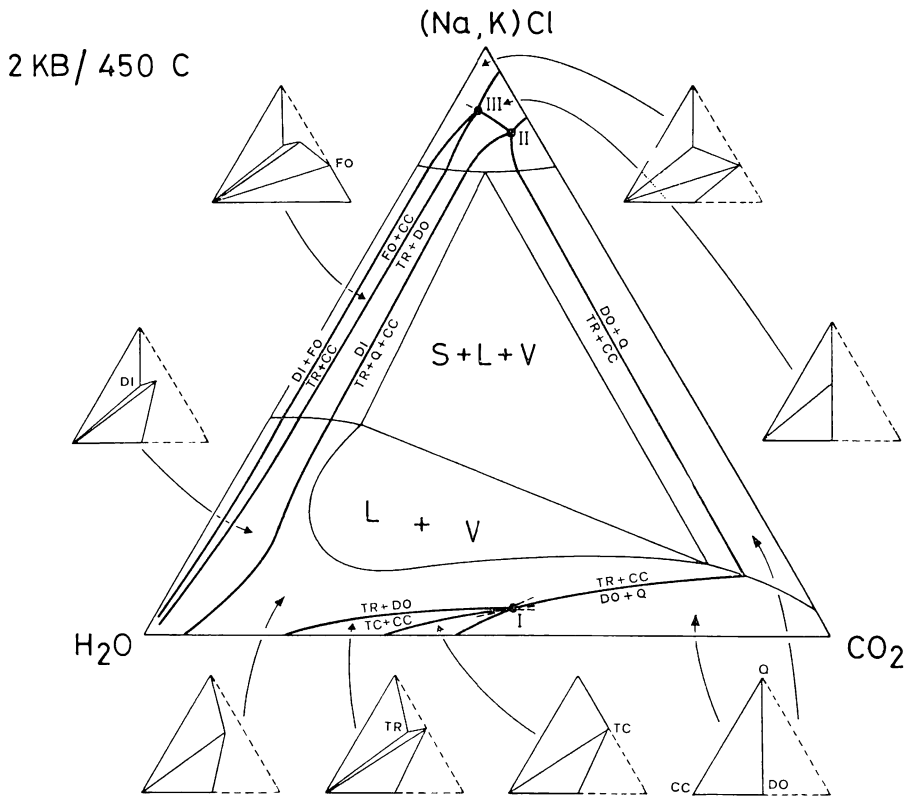


Fig. 12. Relationships at 450°C and 2 kb between mineral equilibria in metamorphosed carbonate rocks and fluids in the system NaCl–KCl–$H_2O$–$CO_2$, as observed at Campolungo, Switzerland. The composition of the salt phase in equilibrium with fluids at Campolungo is at approximately equal molar proportions of NaCl and KCl. The phase elements in the fluid system correspond to those shown in figure 3. Isotherms for carbonate-silicate equilibria correspond to those shown on figures 5 to 7. Phase relations for carbonate-silicate assemblages are shown on triangular diagrams that represent projections onto the CaO–MgO–$SiO_2$ base of the system CaO–MgO–$SiO_2$–$CO_2$–$H_2O$. Only phase assemblages including calcite have been considered as indicated by the triangles drawn with solid lines. Intersections with the binary $H_2O$–$CO_2$ are from Walther and Helgeson (1980). Points labelled with Roman numerals indicate: I: talc–tremolite–quartz–calcite–dolomite; II: tremolite–diopside–quartz–calcite–dolomite; III: forsterite–diopside–tremolite–calcite–dolomite. S = solid solution between KCl–NaCl, L = liquid, V = vapor, FO = forsterite, DI = diopside, TR = tremolite, TC = talc, Q = quartz, DO = dolomite, CC = calcite.

## CONCLUDING DISCUSSION

Figures 12 to 14 illustrate a typical set of relationships between carbonate–silicate assemblages in metamorphic rocks and salt-bearing fluids. These figures are consistent with metacarbonate phase relations in the liquid + vapor ternary element previously derived by Bowers and Helgeson (1983b) for $NaCl–H_2O–CO_2$. Bowers and Helgeson located the liquid–vapor element by analysis of laboratory measurements (Gehrig, 1980) of P–V–T data for supercritical fluids that border the liquid + vapor element. The position of the liquid + vapor element has been determined in a different manner in this study. Free energy data for mineral assemblages observed in the field at Campolungo, Switzerland have been combined with fluid inclusion studies (Mercolli, 1982) and observations of halite and sylvite in these rocks (Trommsdorff, Skippen, and Ulmer, 1985) to locate the halite + sylvite + liquid + vapor element in chemical potential space. An interesting, but not necessarily contradictory, difference between the two approaches is the resulting position of the liquid + vapor element

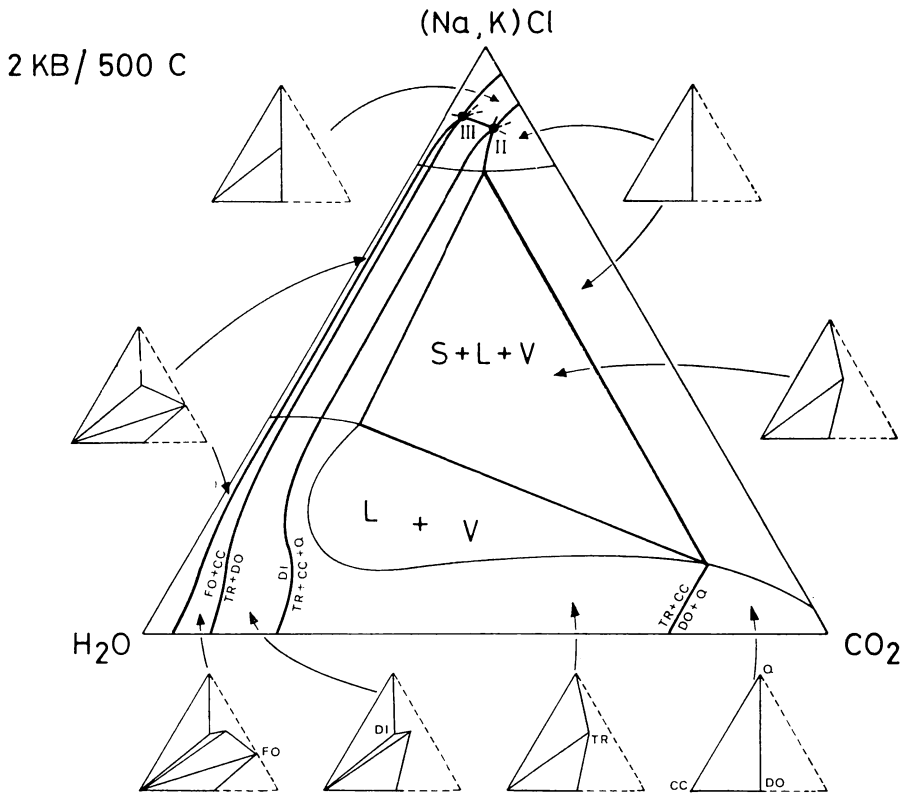


Fig. 13. Relationships at 500°C and 2 kb between mineral equilibria in metamorphosed carbonate rocks and fluids in the system $NaCl–KCl–H_2O–CO_2$, as observed at Campolungo, Switzerland. Diagram is labelled as figure 12.

relative to the binary element in $H_2O$–$CO_2$ for supercritical fluids at lithostatic pressure. The data of Bowers and Helgeson (1983a) suggest that the ternary liquid + vapor element falls outside the binary element on chemical potential diagrams, apparently due to more positive deviation of $H_2O$ and $CO_2$ from ideality in the ternary mixtures. It is also possible that this effect is due to uncertainty in fitting the liquid + vapor phase boundary to limited experimental data. The field data from Campolungo, as interpreted in this work, indicate that the liquid + vapor element for conditions of salt saturation in NaCl–KCl–$H_2O$–$CO_2$ falls beneath the binary curve for supercritical fluid at the pressure and temperature of Campolungo. Phase relations on figures 12 to 14 have been derived on the assumption that the liquid + vapor element remained beneath the binary curve for supercritical fluids at Campolungo.

The phase relations at Campolungo and for the conditions of figures 12 to 14 have been derived with the topology of the salt–fluid system the same as for NaCl–$H_2O$–$CO_2$ under identical conditions as shown on figure

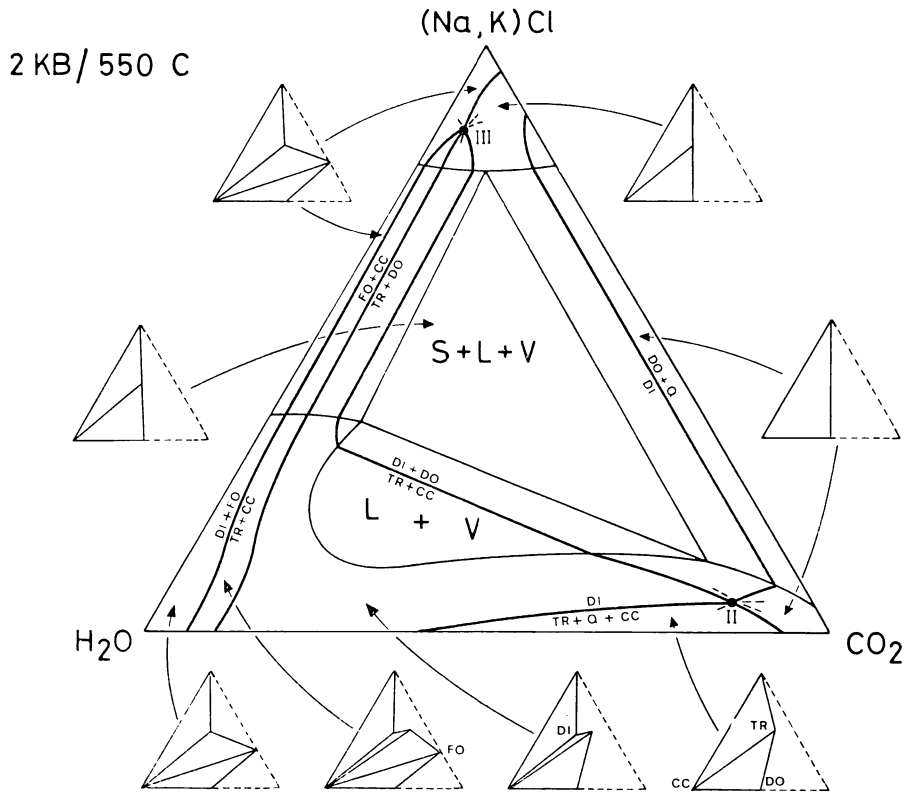


Fig. 14. Relationships at 550°C and 2 kb between mineral equilibria in metamorphosed carbonate rocks and fluids in the system NaCl–KCl–$H_2O$–$CO_2$, as observed at Campolungo, Switzerland. Diagram labelled as figure 12.

1. The information from the rocks of Campolungo supports the assumption that liquid + vapor coexist with salt minerals. It is clear, however, from figures 1 and 2 that other configurations for phase elements in the salt–fluid system are possible. Further correlation of these additional topologies with metacarbonate rocks will proceed as additional laboratory measurements of P–V–T properties of fluids become available and as further field studies of the type described in this paper are carried out over a range of pressure-temperature conditions.

Phase relations such as developed on figures 12 to 14 provide a basis for studying metamorphic processes in carbonate rocks and for understanding more fully the significance of isograds in carbonate rocks that may have been influenced by saline fluids. For example, Masch (ms) has carefully mapped isograds in dolomitic marbles of the Monzoni aureole, Italy. Crossovers of isograds for the appearance of talc and tremolite as well as forsterite and wollastonite have been documented by Masch. It is possible that these relationships between isograds are related to varying salt content of fluids as well as variation in $CO_2$–$H_2O$ ratios. This possibility is enhanced by the intrusion of the Monzoni complex at a depth of only a few hundred meters beneath the sea.

Addition of salt to $H_2O$–$CO_2$ fluids may significantly increase or decrease the stability of certain mineral assemblages in fluid composition space. For example, the assemblage diopside–dolomite may be stable in fluids with high $H_2O$ and NaCl contents, as suggested on figure 14. This assemblage has often been correlated with $CO_2$-rich fluids (for example, Skippen, 1974).

The relationships between mineral assemblages and salt-bearing fluids, as illustrated on figures 12 to 14, also make it possible to understand better geologic processes that involve rock-fluid interaction. Reaction mechanisms and therefore textures in metacarbonates may be influenced by the presence of salt components in the fluids. Reaction paths followed during progressive metamorphism may also be affected by the addition of salt components to the fluids.

The extent of concentrated brines in metamorphic rocks is little known. Trommsdorff, Skippen, and Ulmer (1985) have considered mechanisms that could lead to concentration of salt components. Figure 2 demonstrates the wide P–T range over which ternary fluids in NaCl–$H_2O$–$CO_2$ can exhibit fluid immiscibility. We consider it likely that a $CO_2$-rich fluid dissolves substantially more $H_2O$ than NaCl. Thus, brines in metacarbonate and other $CO_2$ reservoirs could become concentrated in salt components by the separation of a large mass of $CO_2$-rich fluid if such a process occurs on a large scale.

It is therefore increasingly advantageous to study carefully solid and fluid inclusions in metamorphosed carbonates to understand the genesis of these rocks.

ACKNOWLEDGMENTS

This research has benefited from reviews and discussions with our colleagues, Teresa Bowers, Hans Eugster, Hugh Greenwood, and Jacques

Touret. We thank Brigitte Buehlmann and Mona Jakobsson for assistance with manuscript preparation. Financial support has been provided by the Natural Sciences and Engineering Research Council of Canada (Grant A 4253 to G.S.) and the Schweizerischer Nationalfonds (Grant 2.682-0.82 to V.T.).

## REFERENCES

Akella, J., Vaidya, S. N., and Kennedy, G. C., 1969, Melting of sodium chloride at pressures to 65 kb: Phys. Rev., v. 185, p. 1135-1140.

Bowen, N. L., 1940, Progressive metamorphism of siliceous limestone and dolomite: Jour. Geology, v. 48, p. 225-274.

Bowers, T. S., and Helgeson, H. C., 1983a, Calculation of the thermodynamic and geochemical consequences of nonideal mixing in the system $H_2O$–$CO_2$–NaCl on phase relations in geologic systems: Equation of state for $H_2O$–$CO_2$–NaCl fluids at high pressures and temperatures: Geochim. et Cosmochim. Acta, v. 47, p. 1247-1275.

———— 1983b, Calculation of the thermodynamic and geochemical consequences of nonideal mixing in the system $H_2O$–$CO_2$–NaCl on phase relations in geological systems. Metamorphic equilibria at high pressures and temperatures: Am. Mineralogist, v. 68, p. 1059-1075.

Bruton, C. J., and Helgeson, H. C., 1983, Calculation of the chemical and thermodynamic consequences of differences between fluid and geostatic pressure in hydrothermal systems: Am. Jour. Sci., v. 283-A, p. 540-588.

Burruss, R. S., 1981, Analysis of phase equilibria in C–O–H–S fluid inclusions, *in* Hollister, L. S., and Crawford, M. L., eds., Fluid Inclusions: Applications to Petrology: Mineralog. Assoc. Canada, Short Course, v. 6, p. 39-74.

Chou, I. M., 1982, Phase relations in the system NaCl–KCl–$H_2O$. Differential thermal analysis of the NaCl–KCl liquidus at 1 atmosphere and 500, 1000, 1500 and 2000 bars: Geochim. et Cosmochim. Acta, v. 46, p. 1957-1962.

Crawford, M. L., Kraus, D. W., and Hollister, L. S., 1979, Petrologic and fluid inclusion study of calc-silicate rocks, Prince Rupert, British Columbia: Am. Jour. Sci., v. 279, p. 1135-1159.

Eugster, H. P., and Skippen, G. B., 1967, Igneous and metamorphic reactions involving gas equilibria, *in* Abelson, P. H., ed., Researches in geochemistry: New York, John Wiley & Sons, v. 2, p. 492-521.

Flowers, G. C., 1979, Correction of Holloway's (1977) adaption of the modified Redlich-Kwong equation of state for calculation of the fugacities of molecular species in supercritical fluids of geologic interest: Contr. Mineralogy Petrology, v. 69, p. 315-318.

Flowers, G. C., and Helgeson, H. C., 1983, Equilibrium and mass transfer during progressive metamorphism of siliceous dolomites: Am. Jour. Sci., v. 283, p. 230-286.

French, B. M., 1966, Some geological implications of equilibrium between graphite and a C–H–O gas phase at high temperatures and pressures: Rev. Geophysics, v. 4, p. 223-253.

Gehrig, M., 1980, Phasengleichgewichte und PVT-Daten ternärer Mischungen aus Wasser, Kohlendioxid und Natriumchlorid bis 3 kbar und 550°C: Ph.D. dissert., Univ. Karlsruhe, Karlsruhe, West Germany (published by HochschulVerlag, Freiburg, Germany).

Goldschmidt, V. M., 1912, Die Gesetze der Gesteinsmetamorphose, mit Beispielen aus der Geologie des südlichen Norwegens: Videnskap. Scri. I, Math. Naturv. Kl No. 22, p. 2-16.

Greenwood, H. J., 1967, Mineral equilibria in the system MgO–$SiO_2$–$H_2O$–$CO_2$, *in* Abelson, P. H., ed., Researches in Geochemistry: New York, John Wiley & Sons, p. 542-567.

Grjotheim, K., Heggelund, P., Krohn, C., and Motzfeldt, K., 1962, On the solubility of $CO_2$ in molten halides: Acta Chem. Scand., v. 16, p. 689-694.

Guilhaumou, N., Dhamelincourt, P., Touray, J.-C., and Touret, J., 1981, Etude des inclusions fluides du système $N_2$–$CO_2$ de dolomites et de quartz de Tunisie septentrionale. Données de la microscopie et le l'analyse à la microsonde à effet Raman: Geochim. et Cosmochim. Acta, v. 45, p. 657-673.

Helgeson, H. C., Delany, J. M., Nesbitt, H. W., and Bird, D. K., 1978, Summary and critique of the thermodynamic properties of rock-forming minerals: Am. Jour. Sci., v. 278-A, 229 p.

Holloway, J. R., 1977, Fugacity and activity of molecular species in supercritical fluids, *in* Fraser, D., ed., Thermodynamics in Geology: Boston, D. Reidel, p. 161-181.

Korzhinskii, D. S., 1959, Physicochemical basis of the analysis of the paragenesis of minerals: New York, Consultants Bur. Enterprises, Inc., 142 p.

Kozlovsky, Y. A., 1984, The World's Deepest Well: Sci. Am., v. 251/6, p. 106-112.

Kreulen, R., 1980, $CO_2$-rich fluids during regional metamorphism on Naxos (Greece): carbon isotopes and fluid inclusions: Am. Jour. Sci., v. 280, p. 745-771.

Kreulen, R., and Schuiling, R. D., 1982, $N_2$–$CH_4$–$CO_2$ fluids during formation of the Dôme de l'Agout, France: Geochim. et Cosmochim. Acta, v. 46, p. 193-204.

Masch, L., 1977, ms, Die Aureole des Monzoni-Intrusivkomplexes (Nord-Italien), ein Model progressiver Thermometamorphose kieseliger Karbonate: Habilitationsschrift, Univ. München, 118 p.

Mercolli, I., ms, 1979, Le inclusione fluide nei noduli di quarzo dei marmi dolomitici della regione del Campolungo (Ticino): Ph.D. dissert. no. 6378, ETH Zürich, Switzerland, 138 p.

———— 1982, Le inclusione fluide nei noduli di quarzo dei marmi dolomitici della regione del Campolungo (Ticino): Schweiz. min. pet. Mitt., v. 62, p. 245-312.

Ohmoto, H., and Kerrick, D. M., 1977, Devolatilization equilibria in graphitic systems: Am. Jour. Sci., v. 277, 1013-1044.

Poty, B. P., Leroy, J., and Cuney, M., 1974, Les inclusions fluides dans les minerais des gisements d'uranium intragranitiques du Limousin et du Forez (Massif Central, France), *in* Formation of Uranium Ore Deposits: Vienna, Internat. Atomic Energy Agency, Proc., p. 569-582.

Sisson, V. B., Crawford, M. L., and Thompson, P. H., 1981, $CO_2$-brine immiscibility at high temperatures, evidence from calcareous metasedimentary rocks: Contr. Mineralogy Petrology, v. 78, p. 371-378.

Skippen, G., 1974, An experimental model for low pressure metamorphism of siliceous dolomitic marble: Am. Jour. Sci., v. 274, p. 487-509.

Skippen, G., and Carmichael, D. M., 1977, Mixed volatile equilibria: Mineralog. Assoc. Canada, Short Course, v. 2, p. 102-125.

Sourirajan, S., and Kennedy, G. C., 1962, The system $H_2O$–NaCl at elevated temperatures and pressures: Am. Jour. Sci., v. 260, p. 115-141.

Takenouchi, S., and Kennedy, G. C., 1964, The binary system $H_2O$–$CO_2$ at high temperatures and pressures: Am. Jour. Sci., v. 262, p. 1055-1074.

———— 1965, The solubility of carbon dioxide in NaCl solutions at high temperatures and pressures: Am. Jour. Sci., v. 263, p. 445-454.

Tödheide, K., and Franck, E. U., 1963, Das Zweiphasengebiet und die kritische Kurve im System Kohlendioxid-Wasser bis zu Drucken von 3500 bar: Zeitschr. Phys. Chemistry, New Folge, v. 37, p. 387-401.

Touret, J., 1981, Fluid Inclusions in high grade metamorphic rocks, *in* Hollister, L. S., and Crawford, M. L., eds., Short course in fluid inclusions: Applications to petrology: Mineralog. Assoc. Canada, Short Course, v. 6, p. 182-208.

Trommsdorff, V., 1972, Change in T-X during metamorphism of siliceous dolomitic rocks of the Central Alps: Schweizer min. pet. Mitt., v. 52, p. 567-571.

Trommsdorff, V., Skippen, G. B., and Ulmer, P., 1985, Halite and sylvite as solid inclusions in high-grade metamorphic rocks: Contr. Mineralogy Petrology, v. 89, p. 24-29.

Waldbaum, D. R., 1969, Thermodynamic mixing properties of NaCl–KCl liquids: Geochim. et Cosmochim. Acta, v. 33, p. 1415-1427.

Walther, J. V., 1983, Description and interpretation of metasomatic phase relations at high pressures and temperatures: 2. Metasomatic reactions between quartz and dolomite at Campolungo, Switzerland: Am. Jour. Sci., v. 283-A, p. 459-485.

Walther, J. V., and Helgeson, H. C., 1980, Description and interpretation of metasomatic phase relations at high pressures and temperatures: 1. Equilibrium activities of ionic species in nonideal mixtures of $CO_2$ and $H_2O$: Am. Jour. Sci., v. 280, p. 575-606.

Wyllie, P. J., 1962, The petrogenetic model, an extension of Bowen's petrogenetic grid: Geol. Mag., v. 99, p. 558-569.